Journal of Computer-Assisted Microscopy, Vol. 10, No. 3, 1998

Axial Superresolution by Oblique Two-Dimensional Nondiffracting cos Beam Illumination

Carlos J. Zapata-Rodríguez,[1] Manuel Martínez-Corral,[1] and Laura Muñoz-Escrivá[1]

Nondiffracting cos beams may be used in the object space of an optical microscope for causing a nonuniform illumination. This irradiance distribution consists in a set of equidistant plane maxima, and therefore the light radiated by the sample decays in its neighborhood. We propose to observe over an object plane coinciding with one of these illumination peaks, which results in a superresolving axial effect. For that purpose, illumination and detection should be oblique processes, and a computer-assisted z-scanning process is needed in order to access the axial structure of a thick object.

KEY WORDS: Axial superresolution; nondiffracting cos beam; oblique illumination.

INTRODUCTION

Conventional optical imaging systems possess a poor depth discrimination because of a blurring in the three-dimensional (3D) image instead of a selective intensity detection (Streibl, 1985). In order to overcome this drawback, we propose to modify the spatial distribution of light in the object space of a conventional image-formation system to attain an enhancement in the axial resolution. For that purpose, we use a Fresnel double prism to transform a plane wave into a nondiffracting cos beam (Rosen *et al.*, 1995), thus generating an illumination irradiance distribution consisting in a set of equidistant plane maxima. When we observe over an object plane coinciding with one of these maxima with the result that illumination and detection are oblique processes, the strength of the light radiated by the sample decays in the neighborhood of the focal plane according to the spatial frequency of the interference pattern, thus obtaining a superresolving axial effect. The light scattered from other maximum-intensity planes in the object space is blurred with an appropriate defocus. In contrast to the confocal scanning technique, where the optical sectioning effect is obtained by means of a nonuniform illumination emerging from an objective lens (Wilson, 1990), the improvement in axial resolution provided by our method does not involve a reduction in the field of view.

ANALYSIS OF THE 3D IMAGE FORMATION

Let us start by considering the 3D image-formation optical system as shown in Fig. 1. A positive lens collimates the coherent radiation generated by a laser source, thus obtaining a uniform plane wave. A Fresnel double prism, FP, transforms the incident plane beam into two tilted uniform plane waves, which interfere with generating a nondiffracting cos beam, which consists in a set of equidistant plane maxima. However, the tilted plane waves have a limited extension due to the finite size of the biprism, which implies that the interference phenomenon is not observed in the whole half-space.

The 3D normalized irradiance distribution in the interference region may be expressed mathematically as (Born and Wolf, 1980)

$$I_{il}(z_o) = \cos^2(2\pi\nu z_o) \qquad (1)$$

[1] Department of Optics, University of Valencia, Dr. Moliner 50, E-46100 Burjassot, Spain. E-mail: manuel.martinez@uv.es

1040-7286/98/0800-0097$15.00/0

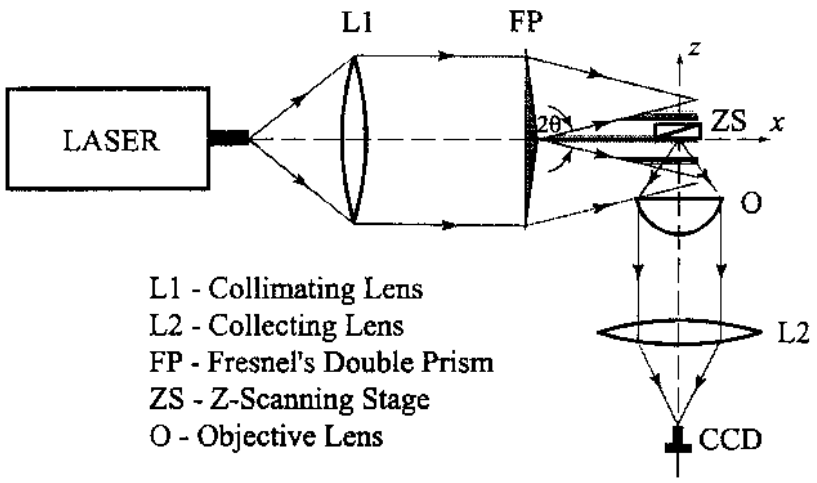

Fig. 1. Schematic diagram of the 3D image-forming system.

where

$$v = \frac{\sin\theta}{\lambda} \tag{2}$$

is the fundamental frequency associated with the interference pattern. We note that this parameter depends on the wavelength λ of the incident radiation and half the angle θ forming both plane waves emerging from the biprism.

The thick sample under observation is then mounted on a z-scanning stage, situated in the interference region of the illuminating beam. If we suppose that the 3D object is scanned to a position z_s, the light field emitted by the sample is given by

$$o(\mathbf{r}_o, z_o + z_s)\cos^2(2\pi v z_o) \tag{3}$$

where we consider a one-photon fluorescence process. Then the light is emitted from the sample with a wavelength λ_f, and $o(r, z)$ describes the light strength of the object fluorescence emission under a uniform illumination. Additionally, we should impose that the observation plane coincides with one of the interference pattern maxima, with the result that illumination and detection are oblique processes, thus constituting a confocal arrangement. Then, the strength of the light radiated by the sample decays in the neighborhood of the focal plane according to the spatial frequency of the interference pattern v, thus obtaining a superresolving axial effect. Finally, the emitted fluorescent light is then driven through an optical microscope consisting in an objective lens with a numerical aperture $\mathrm{NA} = \sin\alpha$, and a collecting lens that focus the light on a Charge-coupled device (CCD).

Now we consider an object in which the scattering is weak so that the first Born approximation is valid (Streibl, 1985). Then, the irradiance distribution in the receiving plane of the digital camera may be expressed in terms of the function

$$I(\mathbf{r}, z_s) = \iiint_{\mathscr{R}^3} o(\mathbf{r}_o, z_o + z_s)\cos^2(2\pi v z_o) \times |h'(\mathbf{r} - \mathbf{r}_o, z_o)|^2 \, d\mathbf{r}_o \, dz_o \tag{4}$$

before a scaling according to the lateral magnification of the optical microscope. In Eq. (4) $h'(r, z)$ stands for the 3D coherent point spread function (PSF) of the objective lens in the object space, and may be given in the paraxial Debye approximation as (Wilson, 1990)

$$h'(r, z) = h(v, u) = 2\int_0^1 \exp\left(i\frac{u}{2}\rho^2\right) J_0(v\rho)\,\rho\, d\rho \tag{5}$$

where

$$u = \frac{8\pi}{\lambda_f} z \sin^2(\alpha/2) \qquad \text{and} \qquad v = \frac{2\pi}{\lambda_f} r \sin\alpha \tag{6}$$

are the spatial axial and radial coordinates, respectively, and J_0 is a zero-order Bessel function of the first kind.

AXIAL SUPERRESOLUTION

According to Eq. (4) the cos-beam illumination z-scanning microscope is a 3D linear shift-invariant

system (Gaskill, 978), having an effective 3D irradiance PSF given by the square modulus of the function

$$h_{\text{eff}}(v, u) = \cos\left(\frac{u}{4}\beta\right) h(v, u) \tag{7}$$

where

$$\beta = \frac{\lambda_f}{\lambda} \frac{\sin\theta}{\sin^2(\alpha/2)} \tag{8}$$

We note that the effective 3D amplitude PSF is comprised of the product of two factors: the first one, which we denote the interference term, arises from the nonuniform cos-beam illumination, and the second corresponds to the 3D amplitude PSF of the objective lens thus it will be named the diffraction term. Then, the diffraction behavior of the system is somehow similar to that of a confocal scanning system, where both the illumination and detection systems contribute to the image formation (Wilson, 1990).

Since the interference term only varies along the optical axis, we may simplify our investigation by considering the axial-irradiance PSF, which for the case of an unapodized objective lens may be written as

$$|h(0, u)|^2 = \left[\frac{\sin(u/4)}{u/4}\right]^2 \tag{9}$$

In Fig. 2 we compare the axial component of the square modulus of the diffraction term, as given in

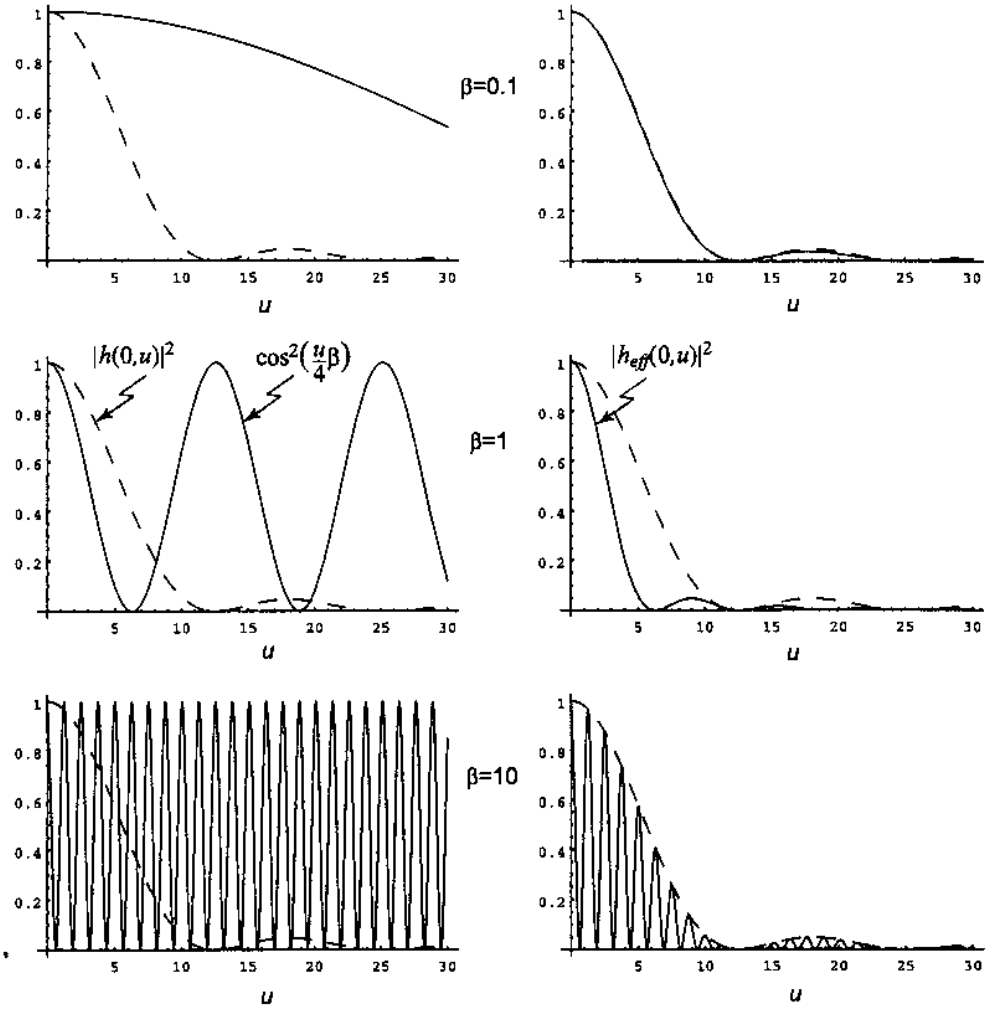

Fig. 2. Comparison of the square modulus of the diffraction term (dashed line), the interference term (left column, continuous line), and the effective PSF (right column, continuous line) along the axis.

Eq. (9), the interference term given in Eq. (1), and the axial-irradiance distribution of the effective PSF, which is obtained as the product of the previous two functions [see Eq. (7)], for different values of β. When this parameter is much lower than unity, the interference term is nearly constant in the focal region, which maintains unchanged the axial resolution of the system. As β comes closer to unity, the period of the interference fringes, given by $1/2v$ ($4\pi/\beta$ in terms of the axial coordinate u), is comparable to the central-lobe width of the objective PSF, i.e.,

$$\Delta z = \frac{\lambda_f}{\sin^2(\alpha/2)} \tag{10}$$

which implies that we have high control over the central-peak width along the axis by simply modifying the frequency of the interference pattern. Finally, when β takes values much higher than unity, the central lobe has a width governed by the period of the interference term, which is much narrower than that of the central maximum of the objective PSF. However, the secondary lobes take high values close to that of the central peak, which limits the gain in axial resolution.

COMPARISON WITH CONFOCAL SCANNING MICROSCOPY

We have deduced previously that the optimum performance of the optical system is then obtained for values of β, close to unity. Specifically, when $\beta = 1$, the axial-irradiance distribution of the effective PSF may be written as

$$|h_{\mathrm{eff}}(0, u)|^2 = \left[\frac{\sin(u/2)}{u/2}\right]^2 = \left|h\left(0, \frac{u}{1/2}\right)\right|^2 \tag{11}$$

that is, the image-formation system with cos-beam illumination has an axial PSF corresponding to that of a conventional optical system with an effective numerical aperture that has been enlarged by a factor $\sqrt{2}$. In other words, the central-lobe width has been reduced to half of its initial value, thus increasing substantially the optical sectioning capacity of the system.

In Fig. 3 we present the 3D PSF of a conventional system, a confocal scanning microscope with two equal illuminating and collecting sets, and a z-scanning imaging system with a cos-beam illumination. We have selected $\beta = 1/2$ in order to demonstrate that the arrangement with a cos-beam illumination behaves as a conventional system along the transversal direction, but has the inherent sectioning capacity of the confocal scanning microscope. For that reason, we may state that the system presented here is hybrid between the conventional and the confocal-scanning imaging systems.

CONCLUSIONS

In summary, we have proposed a new image-formation arrangement with enhanced optical sectioning. Hence, thick objects may be imaged by minimizing a blurring presented in conventional 3D images. In particular, we demonstrate a twofold increase in axial resolution when selecting $\beta = 1$, which is clearly feasible in practical situations. Moreover, optical microscopes may take advantage of this technique by a simply substitution of the illumination system.

Finally, we should emphasize that such arrangement presents several advantages over the confocal scanning technique. First, there exists a higher acquisition speed due to the fact that we acquire a focal series of images, thus showing inherent parallelism.

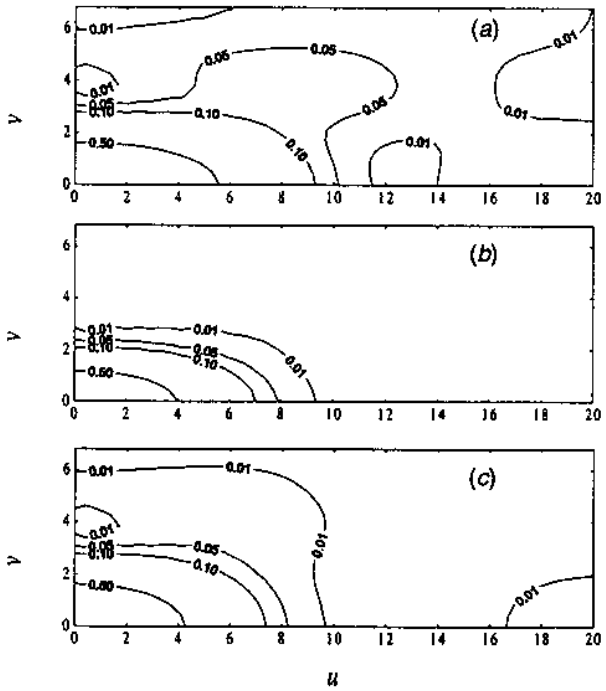

Fig. 3. Isophotes diagram corresponding to the 3D PSF of (a) a conventional, (b) a confocal scanning, and (c) a superresolving z-scanning microscope.

Also, we do not make use of a pinhole in the receiving plane, which produces a great light loss and consequently a low photon efficiency.

ACKNOWLEDGMENTS

Laura Muñoz-Escrivá gratefully acknowledges financial support from the *Cinc Segles* Program, *Universitat de València*, Spain.

REFERENCES

Born, M., and Wolf, E. (1980). *Principles of Optics*, Pergamon Press, Oxford.

Gaskill, J. D. (1978). *Linear Systems, Fourier Transforms, and Optics*, John Wiley & Sons, New York.

Rosen, J., Salik, B., and Yariv, A. (1995). Pseudonondiffracting slit-like beam and its analogy to the pseudonondispersing pulse. *Opt. Lett.* **20**:423–425.

Streibl, N. (1985). Three-dimensional imaging by a microscope. *J. Opt. Soc. Am. A* **2**:121–127.

Wilson, T., ed. (1990). *Confocal Microscopy*, Academic Press, London.